MIR spectral characterization of plastic to enable discrimination in an industrial recycling context: I. Specific case of styrenic polymers

Charles Signoret, Anne-Sophie Caro-Bretelle, José-Marie Lopez-Cuesta, Patrick Ienny, Didier Perrin

MIR spectral characterization of plastic to enable discrimination in an industrial recycling context: I. Specific case of styrenic polymers

Charles Signoret, Anne-Sophie Caro-Bretelle, José-Marie Lopez-Cuesta, Patrick Ienny, Didier Perrin *

C2MA, IMT Mines Ales, Univ Montpellier, 7 avenue Jules Renard, 30100 Ales, France

A B S T R A C T

One of the major limitations in polymer recycling is their sorting as they are collected in mixes. The majority of polymers are highly incompatible without compatibilizers. For sorting of polymers, high-speed online Near-Infrared (NIR) spectroscopy is nowadays relatively widespread. It is however limited by the use of carbon black as a pigment and UV-stabilizer, which strongly absorbs near-infrared signals.

Mid-Infrared (MIR) hyperspectral cameras were recently put on the market. However, their wavelength ranges are smaller and their resolutions are poorer, in comparison with laboratory equipment based on Fourier-Transform Infrared (FTIR). The identification of specific signals of end-of-life polymers for recycling purposes is becoming an important stake since they are very diverse, highly formulated, and more and more used in copolymers and blends, leading to complex waste stocks mainly as WEEE (Waste Electrical and Electronic Equipment). Dark colored plastics are the major part of WEEE, which also contains mainly styrenics (ABS, HIPS and their blends). In addition, styrenics are especially concerned by the need of identification. In this framework, spectral characterizations of ten types of polymers were scrutinized through about eighty pristine and real waste samples. Polymer characteristic signals were aggregated in charts to help rapid and automatized distinction through specific signals, even in limited resolution and frequency ranges.

Keywords:
Polymer recycling
Sorting
MIR
WEEE
Identification
Styrenics

1. Introduction

Plastic waste amounts are growing, as worldwide production went from 322 millions of tons in 2015 to 335 in 2016 (PlasticsEurope Market Research Group (PEMRG) / Consultic Marketing & Industrieberatung GmbH, 2017), especially because of the rise of middle-classes in developing countries and gross domestic product growth (Gundupalli et al., 2017), as they progressively access to lifestyles comparable to the unsustainable ones well established in North America and Western Europe. WEEE (Waste Electrical & Electronic Equipment) plastics, or WEEP, stocks experience one of the fastest growths (Gu et al., 2017; Pérez-Belis et al., 2015) of polymer waste. The global WEEE growth rate is estimated up to 8% by the Bureau of International Recycling ("BIR – Bureau of International Recycling – E-Scrap"), as electronic devices are more and more current in our daily lives, especially in developing countries (Salhofer et al., 2016; Wang et al., 2018), with both the number of devices per consumer increasing and the life spans of these objects decreasing (Soo and Doolan, 2014).

Plastic recycling is not as developed as glass and metal recycling ("*The New Plastics Economy: Rethinking the future of plastics & Catalysing action*", 2017), mainly because of the more complicated mixes of polymers in the waste streams and losses in properties due to impurities and ageing through each step of the life cycle (Hamad et al., 2013; Ragaert et al., 2017). Plastic mixing generally leads to decreased mechanical properties as most of them are incompatible. Therefore, the main technological obstacle to recycling is an efficient and accurate plastic sorting scheme at an industrial scale. In the industry, plastic sorting technologies are currently mainly densimetric separation (sink-float) (Pongstabodee et al., 2008) and NIR (Near-InfraRed) spectroscopy (Beigbeder et al., 2013; Serranti et al., 2011). They are widespread because of their relatively robustness and efficiency (Ragaert et al.,

Abbreviations: **ABS**, Acrylonitrile Butadiene Styrene; **AN**, Acrylonitrile; **ASA**, Acrylonitrile Styrene Acrylic rubber; **ATR**, Attenuated Total Reflection; **ELV**, End-of-Life Vehicles; **FTIR**, Fourier Transform Infrared; **GPPS**, General Purpose Polystyrene; **HIPS**, High Impact Polystyrene; **HSI**, Hyperspectral Imagery; **LIBS** or **LIPS**, Laser Induced Breakdown/Plasma Spectroscopy; **LWIR**, Long Wavelength Infrared (7.4–14.0 μm or 1350–700 cm^{-1}); **MIR**, Mid-Infrared (4000–400 cm^{-1} or 2.5–25.0 μm); **MWIR**, Middle Wavelength Infrared – 2 to 5 μm (5000 to 2000 cm^{-1}); **PB**, Polybutadiene; **PC**, Polycarbonate (from bisphenol A); **PLA**, Polylactic Acid; **PMMA**, Polymethylmethacrylate; **PPE** or **PPO**, Polyphenylene ether or Polyphenylene oxide; **PS**, Polystyrene (GPPS or HIPS); **SAN**, Styrene Acrylonitrile; **SNR**, Signal to Noise Ratio; **St**, Styrene; **UV**, Ultraviolet; **WEEE** or **W3E**, Waste of Electrical & Electronic Equipment; **WEEP**, WEEE Plastics.

* Corresponding author.
E-mail address: didier.perrin@mines-ales.fr (D. Perrin).

2017). Sink-float solution is based on the difference of density between polymers. NIR spectroscopy makes use of hyperspectral imagery (HSI) cameras (Serranti et al., 2010) which create 3D pictures of polymer scraps on a conveyor, the 3rd dimension being a spectrum of the considered pixel. The identified scraps are then ejected in two or three different collecting trays depending of their chemical nature, thanks to a line of compressed air nozzles, the "ejector" seen on Fig. 1.

Unfortunately, waste streams, especially in WEEP, are expected to become even more complex with the use of more blends, copolymers and composites designed to meet the required functional properties. Also, fire standards and elimination of brominated fire retardants (often used in styrenics) due to public regulations in various countries, have urged plastic manufacturers to create more complex set of flame retardant additives, used in for also more complex materials, such as ABS-PC, ABS-PMMA or HIPS-PPE instead of ABS or HIPS (Peeters et al., 2015). This entails overlapping plastic densities (Peeters et al., 2014), limiting sink-float separation. In addition, a great part of ELV (End-of-Life Vehicles) and WEEE plastics are black, mainly for aesthetic and photo-ageing reasons. Hence, carbon black is used as it is relatively cheap, easily incorporated to plastics and widely produced since the beginning of the twentieth century. Regrettably, carbon black strongly absorbs NIR rays, consequently making NIR-HSI inappropriate for sorting these plastics (Beigbeder et al., 2013). In consequence, innovative sorting technologies must emerge.

Sorting technologies issued from the mining industry, as hydrocyclone, froth flotation or jigging, are largely considered in the literature (Censori et al., 2016; Gundupalli et al., 2017; Yuan et al., 2015). Because of their close chemical natures and thus, densities and surface properties, ABS and HIPS cannot be efficiently and economically sorted at an industrial scale with the aforementioned techniques. Optical techniques, especially spectroscopic, are reported as more promising for complex problematics (Vrancken et al., 2017). Among spectroscopic sorting techniques, LIBS has been intensively studied (Ángel Aguirre et al., 2013; Aquino and Pereira-Filho, 2015; Barbier et al., 2013; Costa et al., 2017; Grégoire et al., 2011; Huber et al., 2014). Based on atomic emission caused by plasma atomization, identification is enabled by quantifying emitted species (C2 or CN). Especially, ABS can be differentiated from HIPS because of its nitrogen atom, thus emitting more CN (Barbier et al., 2013). Besides this example and oxygen content, differences can be subtle between polymers and plastic formulations can be misleading, as with every other elemental technology, because of very similar atomic compositions. Also, the viability of industrial solutions is currently limited. Raman is also considered (Roh et al., 2017; Yamaji et al., 2013). This spectroscopy provides information similar to infrared, as vibration energies are studied. But, as the excitation mode is very different, collected signal is weaker, implying high sensibility or powerful sources, which can be problematic for heating issues. More unusual ways were studied, as fluorescence lifetimes differences (Langhals et al., 2014), impact acoustic emissions(Huang et al., 2017) or melted state separation (Dobrovszky and Ronkay, 2014). It is however important to consider different technologies as potentially complementary in a complex sorting scheme (Gundupalli et al., 2017).

MIR is proposed in this study because MIR hyperspectral cameras are already developed at industrial scale and documented in the literature. MIR spectroscopy, especially FTIR (Fourier Transform Infrared), is widely used for analysis in organic and polymer chemistry as the absorbed wavelengths are characteristic of different vibration modes of covalent bonds. Chemists tend to describe the MIR domain widely as 4000–400 cm^{-1} (2.5–25.0 μm). Optic researchers and commercial hyperspectral cameras producers tend to define two subdomains within this range: MWIR, Middle Wavelength Infrared from 2 to 5 μm (5000–2000 cm^{-1}); and LWIR, Long Wavelength Infrared, roughly from 7.4 to 14 μm (1350–700 cm^{-1}). Both these ranges were first used in thermal imagery (Mooney et al., 1997) and were probably adapted to HSI afterwards. It should be emphasized that these definitions are not normalized, vary between manufacturers and could change in the future.

In addition to shorter operating ranges, Hyperspectral Imagery is subject to other limitations, in comparison with laboratory FTIR. The first one is the acquisition time: whereas a spectrum is often acquired in several seconds to enable good signal-to-noise ratio (SNR) by performing more than a dozen scans, HSI cameras used in an industrial recycling context must lead to identification within a few milliseconds to enable sorting through compressed air nozzles activation, as conveyors go usually at several meter per second. Such a high output is mandatory to make the sorting step economically viable in the industrial recycling context. Also, whereas laboratory infrared sources are punctual and can be weak since analysis is made in contact, industrial applications need strong sources similar to radiant heating systems as analysis is remote. Heating issues must

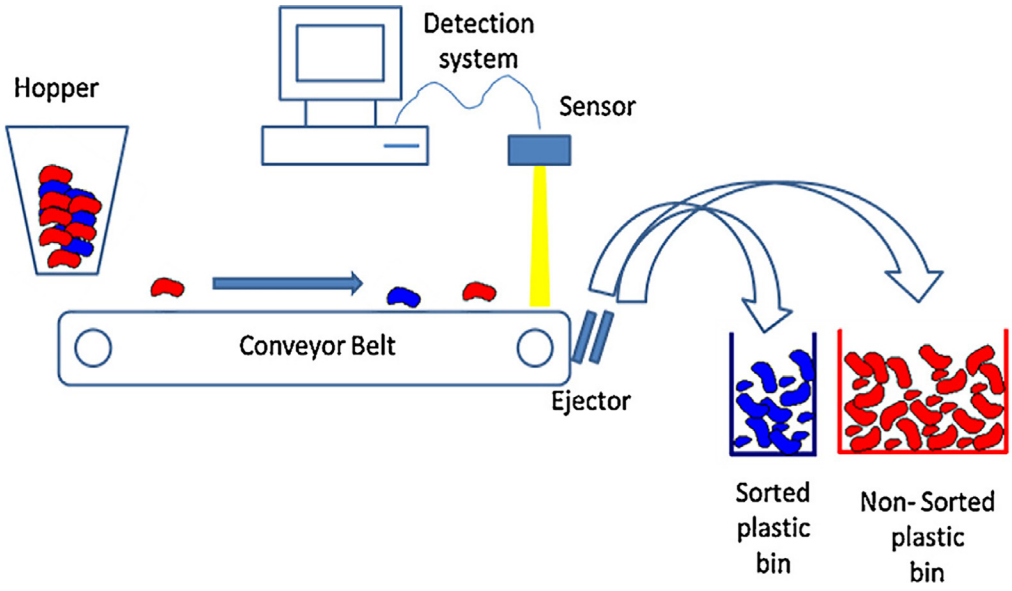

Fig. 1. Principle of optical sorting – e.g. NIR HSI.

be assessed and foster to use high speeds for conveyors. Another limitation of HSI is resolution. Whereas FT-IR spectrometers are equipped with Michelson interferometers in which wavelengths can be finely scanned, HSI cameras have a limited number of spectral channels for each pixel. Each channel is associated to a subpixel and their number is thus technologically and economically limited. Finally, both these technologies share limitations with other optic/spectroscopic techniques: only the surface is analyzed and is thus subject to ageing, dirtiness, degradation, paint or coating; relatively diluted species as flame retardants, plasticizers, minor components of a blend can be difficult to perceive.

The goal of this first study is to transpose NIR HSI spectrum analysis to MIR HSI, an emerging technology which could help sorting black plastics. A few papers have been published about plastic discrimination thanks to MWIR (Kassouf et al., 2014; Rozenstein et al., 2017). However, they mainly discussed about technology and/or computational matters, as models of HSI cameras and/or development of algorithms to enable automatized discrimination. They also considered only materials which are not the main ones connected to industrial current issues, e.g. PLA which represents at this moment a negligible waste stock. This study proposes an innovative overview of the joint consideration of polymer distinction within MWIR, LWIR and MIR more focused on physical-chemistry analysis to serve as a proof of concept for a wide and detailed range of polymers actually found within the considered waste stocks. A complex waste stream of WEEP is thus examined, containing more engineering plastics, mainly styrenic polymers and their blends. As HSI is strongly limited in comparison with FTIR, it seems important to be rather exhaustive in laboratory characterization, not to put aside a signal which could make the difference. This is why every peak in the whole wavelength range of MIR was considered, whereas most of literature is focused on reduced ranges for simplification and clarity. This study is also devoted to waste characterization at laboratory scale, as we tried to point out some unusual materials easily mistaken for other chemically close polymers, especially in the case of degraded acquisition conditions due to limited resolution, unfavorable surface aspect, and occurrence of additives or fillers. Described signals were also checked within real waste samples to assure that they were characteristic of the polymer, and not formulation or ageing. Considerations thus go from a global scale to a rather detailed state and extrapolations to industrial systems about automated decision reliability must be adapted to their respective performances, especially as they will progress in the future.

A second paper will deal with polyolefins: PE and PP, as they are the second most important part of WEEP. In addition, they are very detrimental to styrenic properties as impurities upon recycling. A third work of spectral characterization will be done on the impact of depreciated acquisition parameters and formulation (especially carbon black, fillers and flame retardants) on polymer identification as WEEP and ELV plastics are especially concerned by black plastics sorting issues. A fourth work is about the impact of photodegradation on spectral features of styrenics, polyolefins and polycarbonate and possible repercussions on identification.

2. Materials and methods

2.1. Materials

The types of polymer standard samples considered in the overall project were decided after bibliographic researches but also from analysis of real waste samples provided by Suez company (France). This first study was focused on styrenic materials encountered in WEEE streams, which are principally represented by ABS (acrylonitrile-butadienestyrene) and HIPS (High Impact Polystyrene). These two polymers are derivatives of respectively SAN (styrene-acrylonitrile) and GPPS (general purpose polystyrene or PS crystal). They are often blended with technical polymers as PC (polycarbonate), PMMA (poly methyl methacrylate) or PPE (polyphenyl ether). Virgin plastic references used in pellets to produce standard samples are presented in Table 1:

Some samples from a collection of industrial materials standards called the "Materiautech", a service provided by Allizé-Plasturgie ("Allizé-Plasturgie: a professional organisation at the service of plastics and composites | Allizé-Plasturgie," n.d.) were analyzed for complementary information. This was done when concerned materials were unavailable at the laboratory in pellet form or to check potential composition ratios variations for blends and/or copolymers (Table2):

112 waste samples were kindly provided by the Suez company from their plants in Feyzin (SITA) and Berville-sur-Seine (NORVAL) in France. 43 of them were selected as whole objects or fragments from WEEE. The 69 others were scraps issued from grinding mills. About a third was from casings of cathodic and flat screens. The rest was from a sinking fraction of municipal waste deposits and WEEP. Most of them could not be identified by NIR technology. They are mainly dark colored, unmarked or exhibit bad surface aspect. More than half of them were styrenics and their spectra were analyzed for this work.

2.2. Micro-injection

Small disks, with a diameter of 25 mm and a thickness of 1.5 mm, were injected to serve as virgin standard samples. They

Table 1
List of polymer pellets references.

Polymer	GPPS	HIPS	HIPS	ABS	ABS	ABS	ABS	SAN	SAN	ASA	ASA	ABS-PC	PC	PMMA
Commercial name	PS crystal 1340	Polystyrol 485I	Polystyrol 495F	Terluran GP-22	Terluran GP-35	Terluran HI-10	Novodur H701	Luran 388 S	Luran 368 R	Luran S 757G	Luran S 778T	CM404 - Stapron C	Makrolon 2808	Altuglas V825T
Company	Total	BASF					Styrolution					DSM	Bayer	Arkema

Table 2
List of used "Materiautech" references.

Polymer	HIPS/PPE	HIPS/PPE	SAN	SAN	ASA	ABS/PMMA	SMMA
Reference	I/37	I/42	I/293	I/312	I/111	I/291	I/295
Commercial name	Noryl Resin 731	Noryl Resin FXN119BK	Tairisan NF200	Tyril 905	KIBILAC PW-978B	Tairilac AT5500	NAS 21
Company	Sabic		Formosa Chemicals & Fibre Corp.	Styron	CHI MEI	Formosa Chemicals & Fibre Corp.	Styrolution

were produced thanks to a Zamak-Mercator injection molding machine. Closer to small-scale transfer molding, this equipment allows to work on a few grams of pellets. This form was chosen for reproducibility of ATR spectra as every disk has a similar surface aspect, flat and smooth enough for good detection.

2.3. FTIR-ATR spectroscopy

A Vertex 70 FT MIR spectrometer from Bruker with an ATR unit was used. The used resolution was of 4 cm^{-1}, 16 scans for background acquisition and 16 scans for the sample spectrum. Spectra were acquired from 4000 to 400 cm^{-1} and analyzed thanks to the OPUS software provided with the spectrometer. Most of samples were directly analyzed on the crystal. Some of them needed to be cut to get a smooth enough surface for a good acquisition of the spectrum. Standard samples and very dirty waste samples were cleaned with ethanol.

FTIR-ATR (Attenuated Total Reflection) was chosen for convenience and to be closer to the industrial conditions of HSI cameras. Indeed, both techniques are reflective and can be used directly on solid samples. The industrial application is obligatory reflective as nearly all of samples are opaque to infrared rays. Technologies based on reflectivity have strong sensibility of surface condition, especially labels, paint and dirtiness. However, ATR and HSI main difference is that the first one is made with contact with the sample whereas the second is remote. ATR is thus very sensible to flatness and roughness of the sample whereas HSI is less. However, the major part of encountered difficulties to obtain a understandable spectrum were related to surface quality.

3. Results and discussion

3.1. Presentation of the styrenic family

All styrenic polymers contain styrene (St) as one of their monomers, hence the name. GPPS (General Purpose Polystyrene) is the simplest of all, consisting only of styrene. SAN is a random copolymer of acrylonitrile (AN) and styrene (St). As both PS and SAN are fragile, slightly crosslinked polybutadiene (PB) is added to their formulations to respectively produce HIPS (High Impact) and ABS (Acrylonitrile Butadiene Styrene), which have better impact resistances. As PB is immiscible to these matrices, it creates nodules (Forest et al., 2015). As this elastomeric phase is sensitive to aging because of its residual double bonds, outdoor applications require rather ASA than ABS, where PB is substituted by acrylic rubber (Tolue et al., 2009), which corresponds to the second A of ASA.

Because of their ductile behavior and processing easiness, they can be blended with more technical polymers (Utracki, 1998). Therefore, ABS-PC is widely found in WEEE. HIPS-PPE (polyphenylene ether or PPO, polyphenylene oxide; also called PPE/PS) and ABS-PMMA are also found in smaller amounts which could highly increase in the future (Peeters et al., 2015). These blends are particularly used in the automobile industry.

The most remarking patterns of styrenics (Fig. 2) are the two aliphatic CH stretching signals at 2920 and 2850 plus the 3–5 aromatic CH stretching signals between 3000 and 3100 in MWIR and the two aromatic CH waging at ≈700 and ≈750, the second one at one third of the height of the first one at the lowest wavenumber limit of LWIR.

3.2. Spectra comparison methodology description

To help polymer discrimination, all the charts were built by computing most of the signals seen on the spectra both in MWIR (Table 3) and LWIR (Appendix B) ranges. Each line is attributed to a polymer nature and lines are organized by chemical closeness. Peaks were aggregated in each column when they were 10 cm^{-1} close to each other: signals in the "1375" column should be at 1375 ± 5 cm^{-1}. Most of values are averages of wavenumbers from standards and waste samples when several ones were available. No empty column was constructed. Therefore, two adjacent columns can have a very close or very far wavenumber difference (e.g. 850–840 and 2720–2510). Colors show subjectively the relative intensity of a signal, in comparison with the strongest peak of the considered range. Three levels were chosen: red for the strong ones, orange for moderate and yellow for weak ones. Pale yellow is also used for especially hard-to-see signals. In the case of shoulders and convoluted signals, the color is more associated to how well the peak was seen than to the real height of it.

Thanks to these charts, signals characteristic to certain polymers can easily be identified. Most of the discussion on polymer distinction in this work is largely based on these charts which highlight specific peaks, then comforted by spectra direct visual comparisons. The spectra of the ten considered references are available in Appendix A.

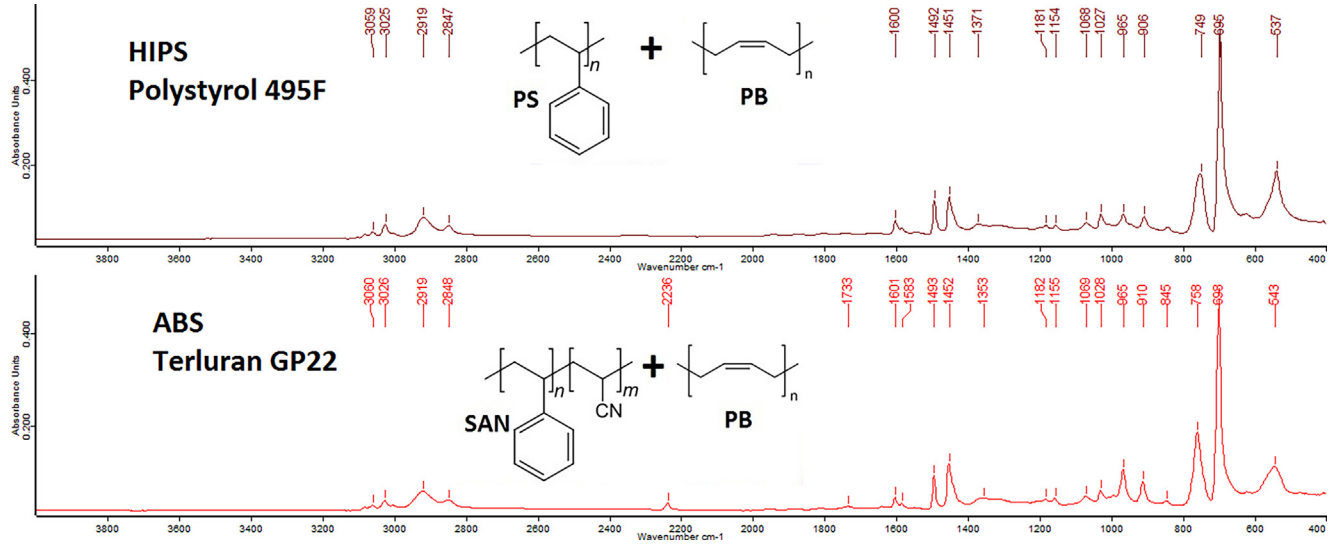

Fig. 2. MIR spectra of reference samples of HIPS and ABS.

Table 3
Signals of styrenics and their blends in MWIR.

	Polymer	3080	3060	3040	3025	3000	2995	2965	2955	2930	2920	2870	2850	2735	2240
PS based	GPPS	3081	3059		3025	3002					2920		2849		
	HIPS	3081	3059		3025	3002					2920		2849		
	HIPS/PPE	3081	3059		3025	3002					2920		2849	2735	
SAN based	SAN	3083	3061		3026	3003					2923		2854		2237
	ABS	3083	3061		3026	3003					2921		2851		2237
	ASA	3085	3060		3027	3003			2957	2929		2874			2237
	ABS/PMMA		3063		3026		2990		2950		2922		2847		2237
	ABS/PC		3060		3027			2967		2926		2872	2852		2237
Other	PMMA						2993		2950		2922		2848		
	PC		3058	3040				2967		2932		2871			

The MWIR chart (Table 3) was limited between 3080 cm^{-1} and 2240 cm^{-1} as no significant signals were seen elsewhere for the chosen polymers. The LWIR chart in Appendix B was intentionally built with a slightly wider range than commercial ones to show that it could be highly profitable that LWIR HSI cameras extend their wavenumbers ranges. Indeed, very interesting signals can be observed just below (aromatic CH bending at 700) and just above (CH_2 and CH_3 bending about 1400 and moreover the C=O stretching from 1550 to 1800 depending on its chemical environment).

When compared to the one hundred of waste samples, the MWIR and LWIR charts were proven to be representative and very helpful in polymer discrimination, especially as most peaks wavenumbers turn out to be very reproducible and rather specific of polymer nature, even within 5 cm^{-1}.

3.3. Styrenic polymers and copolymers: GPPS, HIPS, SAN, ABS and ASA

The main difference in MWIR between ABS and HIPS is the acrylonitrile carbon-nitrogen triple bound stretching which produces a pretty weak but sharp signal at 2230 cm^{-1}, a very specific location (Fig. 3). There is also a difference in aliphatic/aromatic intensities on each side of 3000 cm^{-1}. Whereas aromatic and aliphatic signals are almost at the same level in GPPS, aliphatic are slightly stronger in HIPS as it contains PB, thus, more aliphatic CH. It is also the case with SAN compared to GPPS as it contains AN. It is even more

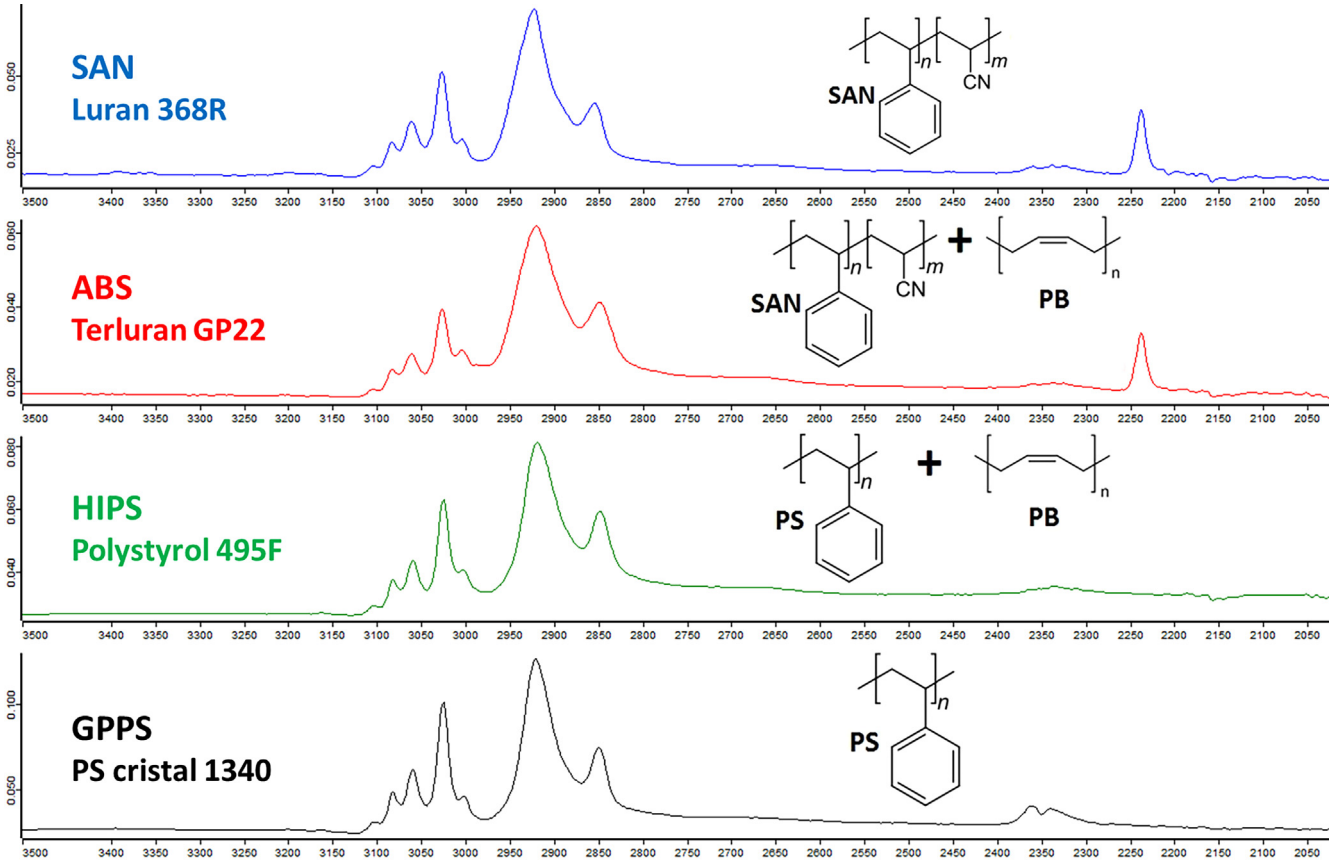

Fig. 3. GGPS, HIPS, SAN and ABS reference samples in MWIR.

marked with ABS as it contains both PB and AN. These height ratios differences were not retrieved within real waste samples, as ageing, blending and formulation affect them. Only the acrylonitrile peak is thus reliable for distinction in this range, especially in degraded conditions, and PB is undetectable.

In the LWIR range (Table 4 and supporting information), one of the two St signals (aromatic CH bending) was found at 750 ± 4 for the forty PS based samples (GPPS, HIPS, HIPS-PPE) but around 759 ± 3 for the twenty-five SAN based samples (SAN, ASA, ABS-PMMA, ABS and ABS-PC). Similarly, the other St signal was at found at 695 ± 2 for PS based samples but at 700 ± 3 for SAN based polymers (as highlighted by dotted lines on Fig. 4). It can be deduced that the presence of acrylonitrile in the polymer chains affect the aromatic C-H vibrations. This difference was proved to be more reliable than the acrylonitrile peak at 2230 since it can be hard to detect in case of limited SNR, due to bad acquisition conditions as a non-flat rough surface, or in case of reduced intensity due to blending as discussed in part 3.4 with ABS/PC.

Another difference within styrenics is due to varying amounts of PB within the different polymers (Fig. 4). As reported by Saviello et al. (2014), PB has only a few signals, with only two easily seen in LWIR at 965 and 910 cm^{-1}. Sadly, the second one is superimposed with a styrene specific signal. As expected, pristine styrenics grades with higher impact strengths (but slightly lower modulus and higher viscosities) often display stronger PB signals. Generally, ABS samples seem to contain more elastomeric parts than HIPS ones, which can be linked to commonly better impact strengths. Indeed, ABS is reported to contain between 5 and 30 w% of PB (Wypych, 2016a) whereas HIPS rates would usually be from 6 to 8.5 w%, with highest ones limited at 15 (Alfarraj

Table 4
Some LWIR signals typical of St and PB in the styrenic family and their blends.

	Polymer	1185	1160	1140	1075	1015	960	910	850	840	830	760	750	700	690
PS based	GPPS							906		841			749		694
	HIPS						965	906		841			749		695
	HIPS-PPE	1183				1019	958	906	855		830		752		696
SAN based	SAN							910		845		759		698	
	ABS						965	910		845		758		699	
	ASA		1161		1068		964	912		842		761		699	
	ABS-PMMA			1141	1075		965	910		842		758		701	
	ABS-PC	1187	1158		1080	1013	965	911			828	757		700	
Other	PMMA	1189		1142			964	912		840			750		
	PC	1187	1158		1079	1013					828				

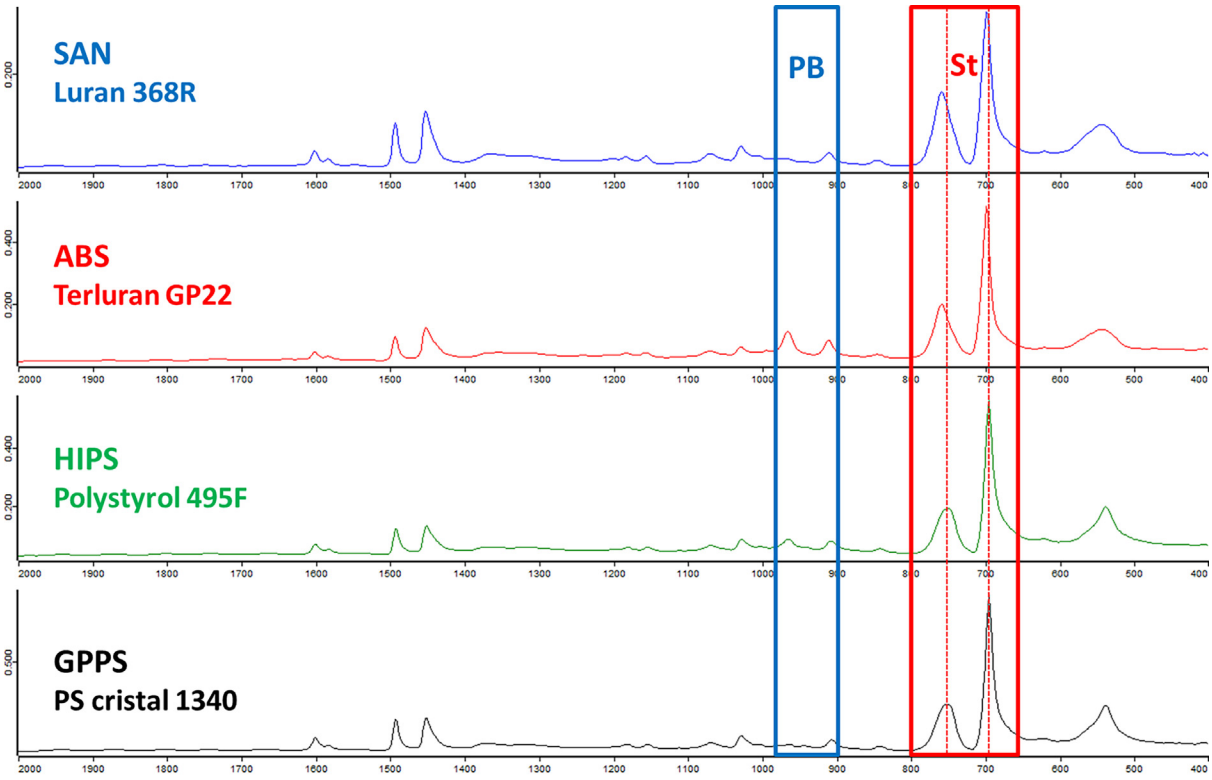

Fig. 4. Presence of PB (framed in blue) and shifts in St CH peaks (framed in red) due to AN in styrenics – LWIR – vertical dotted lines placed on PS peaks at 695 & 750 cm-1. (For interpretation of the references to colour in this figure legend, the reader is referred to the web version of this article.)

and Bruce Nauman, 2004). Higher amounts of PB can also explain why aliphatic signals are stronger than aromatic ones in MWIR for ABS than HIPS samples.

However, these PB signals are often hard to see, as on Fig. 5, where waste sample "EN2" displays a surface spectrum closer to GPPS than HIPS. As numerous others, it was however identified as HIPS as it was ductile and not fragile when cut. Waste sample "EN5" is among the few exceptions as its spectrum displays PB peals. ABS waste samples display similar behavior towards SAN and ABS references. As PB is often the key parameter in styrenics ageing (Arnold et al., 2009; Vilaplana et al., 2006), it is often the first oxidation target and its spectral signature rapidly disappears from the surface.

ASA is spectrally different from other styrenics. The two main signals below 3000 seem shifted to the higher wavenumbers (Fig. 6). In fact, the SAN signals are partially masked by the stronger ones of butyl acrylate. As this phase is chemically close to PMMA, we observe a spectral resemblance, luckily only partial, which thus preserves differentiation. PMMA displays a supplementary signal at 2990 cm^{-1}, which is rather high for an aliphatic C-H stretching in polymers. In PLA, this wavenumber has been attributed to CH stretching of CH_3 (Kister et al., 1998). We can go further and

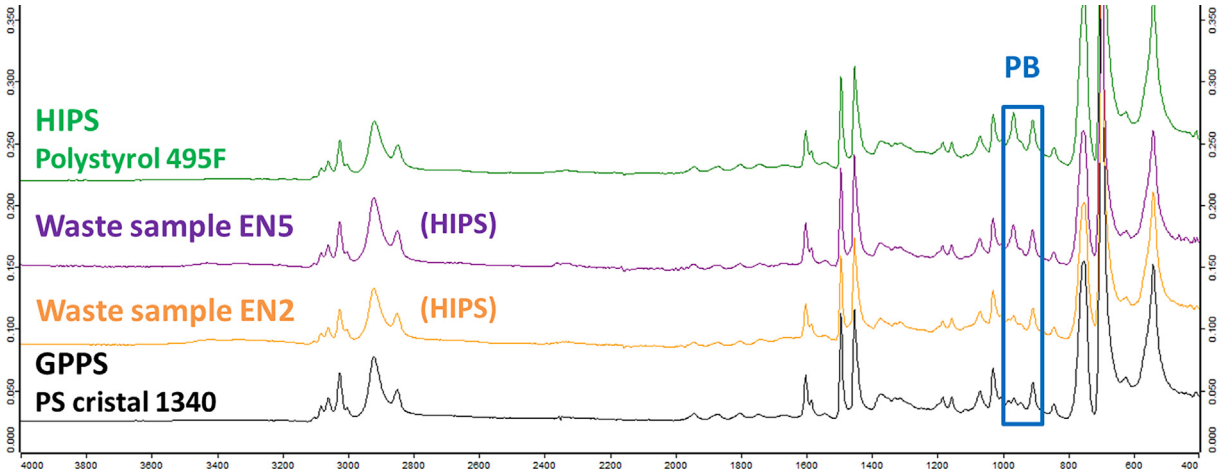

Fig. 5. MIR spectra comparison of HIPS real waste samples to GPPS and HIPS references to highlight PB disappearance (framed).

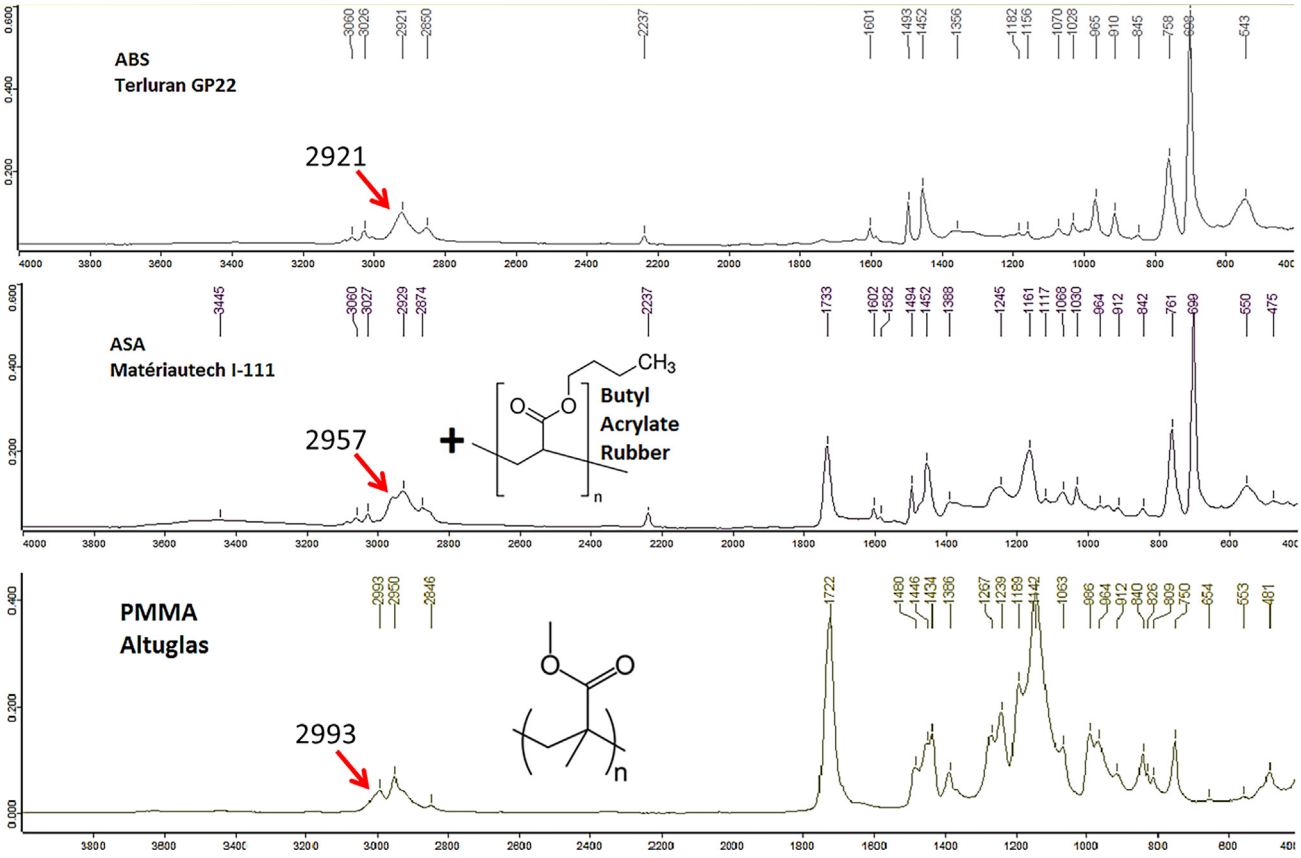

Fig. 6. MIR comparison of reference samples of ASA, ABS and PMMA – highest aliphatic C-H stretchings arrowed.

suppose that it is specifically associated to CH_3 groups in alpha position of an ester function. However, no ASA waste sample was found among the studied waste stock, but ABS-PMMA blends discussed below, spectrally reminiscent but different.

For thermal stability, α-methylstyrene can substitute a part of styrene in ABS or ASA formulations (Utracki, 1998). It is the case with Novodur H701 (Fig. 7). The most notable spectral difference is a band at 1388 whereas regular ABS rather has a mount culminating at 1353 cm^{-1}. This signal is close to 1375, generally associated to C—H bending in CH_3 groups, as in PP. It also leads to stronger intensities of aliphatic C—H stretching signals between 2800 and 3000 cm^{-1}. These differences were too subtle to enable alpha-methylstyrene detection within waste samples (blended, aged, formulated and with rough surfaces) even at laboratory scale. However, these polymers are unlikely to be incompatible with their "non-thermal" counterparts. This difference is also visible in ASA (Fig. 8).

PS-based (HIPS and GPPS) and SAN-based (SAN, ABS, ASA and methyl-styrene copolymers) polymers can be differentiated mainly through to the acrylonitrile peak in MWIR, however not very intense. It is thus essential to achieve a good sensibility in its zone (2237 cm^{-1}) and also sufficient resolution as carbon dioxide signals are relatively close, roughly 2400–2300 cm^{-1}. They also differentiate in LWIR through the exact positions of aromatic C—H deformations (695 + 750 for PS, 700–760 for SAN). These signals are however at the limit of LWIR, even out of range for several commercial HSI cameras. PB is hardly detectable in both MWIR and LWIR, especially as it is strongly subjected to oxidation. However, almost every encountered waste samples were impact-modified (only one SAN and no GPPS) as they were ductile. Incompatibility between GPPS and HIPS is limited (Perrin et al., 2016), if not inexistent, especially at these proportions. Same behavior is to be expected from SAN toward ABS. ASA is sufficiently spectrally different to be detected in both MWIR and LWIR but was not encountered within the waste stock. Finally, "thermal" alpha-methylstyrene copolymers display very minor spectral modifications which are hardly perceived, even at laboratory scale, but compatibility issues are not to be expected.

3.4. Styrenic blends: PPE-PS, ABS-PC and ABS-PMMA

In the MWIR range, PPE-PS (in fact HIPS-PPE) has stronger aliphatic CH signals (3000–2800) compared to aromatic ones (3100–3000) than pure HIPS (Fig. 9). This can be explained by the fact that most PPE are made from dimethylphenol (Wypych, 2016b). As aromatic CH bonds have weaker absorption coefficients than aliphatic ones, the CH_3 groups of PPE contribute more to the 3000–2800 signals whereas its aromatic CH contributes to the 3100–3000. Also, there is a slightly visible shoulder at the left side of the 2920 peak and a very weak signal at 2735 which is barely perceptible, not seen on all samples, especially waste samples, surely because of varying spectra qualities and various ratios of

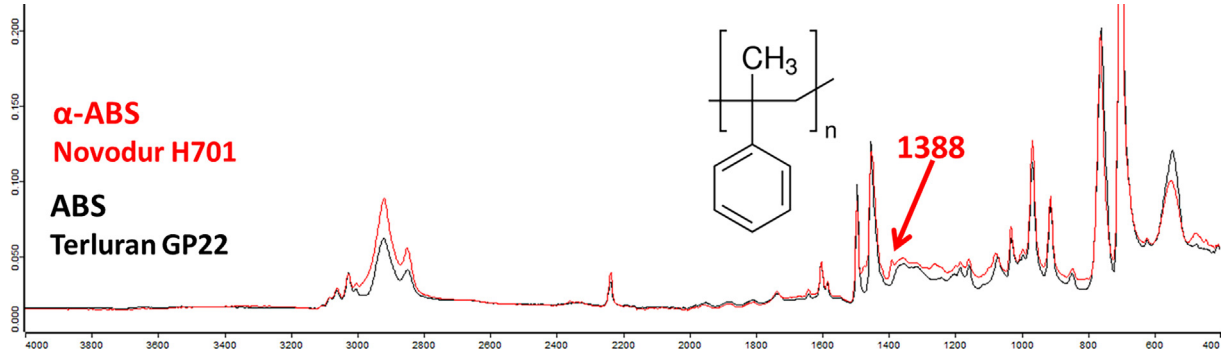

Fig. 7. MIR comparison of reference samples of standard ABS and ABS containing α-methylstyrene – main difference arrowed.

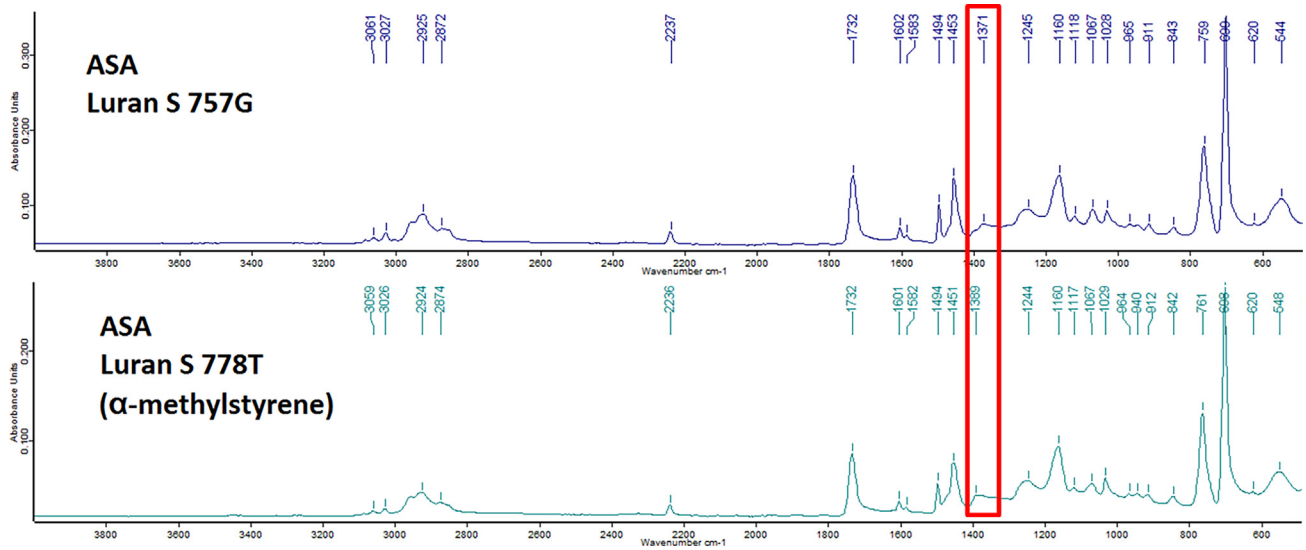

Fig. 8. MIR comparison of reference samples of standard ASA and ASA containing α-methylstyrene – main difference framed.

PPE and HIPS. These subtle differences were also retrieved on waste samples (“EN2” and “CC2” on Fig. 9) but are not expected to be seen industrially because of sensibility and resolution reasons.

In LWIR range (Fig. 10), HIPS/PPE has a lot more signals than pure HIPS, especially at 1180 cm^{-1} for C—O stretching. Ratios between signals characteristic of HIPS and those of PPE can be subject to variation as they are compatible on a wide range (Yee, 1977). However, the six samples identified as HIPS-PPE displayed spectra similar to the reference as “CC5” shown on Fig. 10. As one could overlook the 1500–800 cm^{-1} and just pay attention to MWIR, C═O and St signals, HIPS-PPE can be mistaken for regular HIPS at laboratory scale.

According to these results, HIPS and HIPS-PPE are not expected to be industrially differentiated through MWIR. LWIR could enable identification but peaks richness could negatively impact it, especially through convolution at low resolution and as it means more consequent data treatment. Indeed, high output of sorting machines means high acquisition time but also high calculation time. Having more data to handle can be thus critical for performance. Within the studied waste stock, one sample was identified as HIPS-PPE for every five HIPS ones. No PPE alone was found, concordantly with the fact it is very rarely commercialized alone. As HIPS and PPE are widely compatible, confusing them is not critical, even if it means being enable to valorize HIPS-PPE at its maximal potential.

ABS-PC is widely used in WEEE and the weight ratio between PC and ABS is usually 70/30 as it leads to the best performance in both tensile and impact properties (Greco et al., 1994). The distinction in LWIR between ABS-PC and pure PC can be done thanks to the PB signal at 965 and the St ones at 760 and 700 cm^{-1}, absent on pure PC (Fig. 11). As well, signals of the PB phase from ABS are visible at

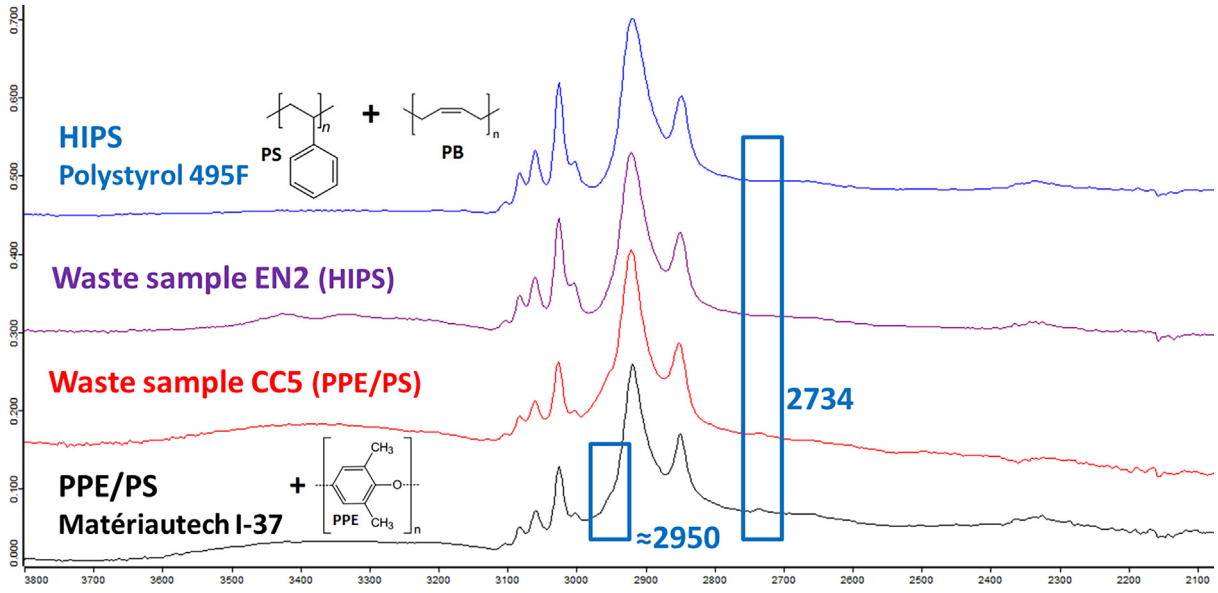

Fig. 9. Differences (framed) between PS and PPE/PS in MWIR – a reference and a waste sample for each material nature.

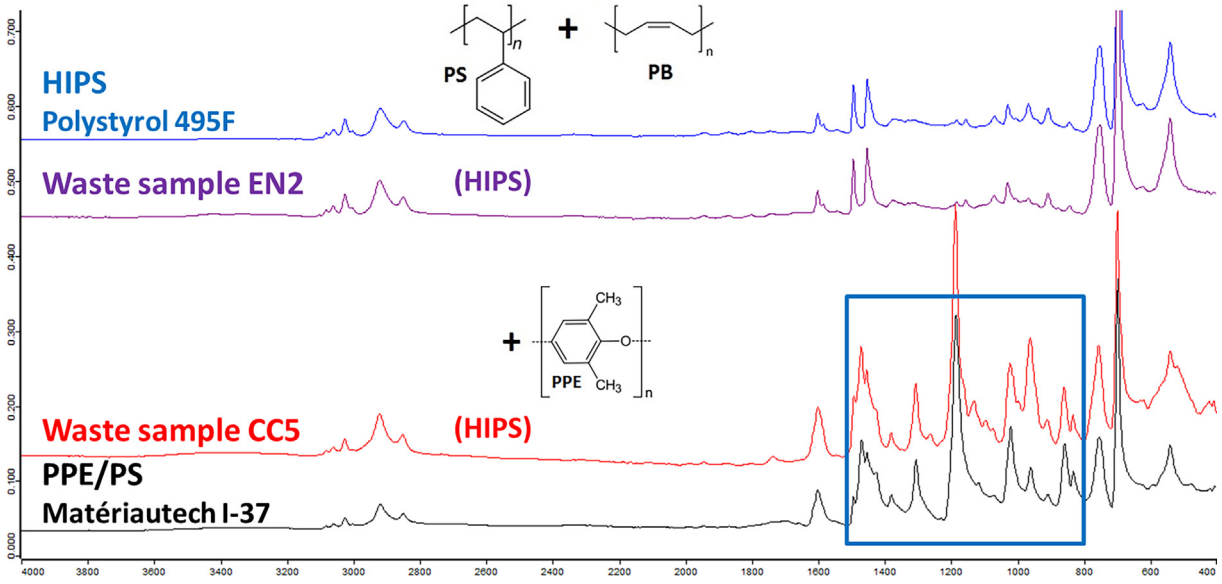

Fig. 10. Differences (framed) between PS and PPE/PS in MIR – a reference and a waste sample for each material nature.

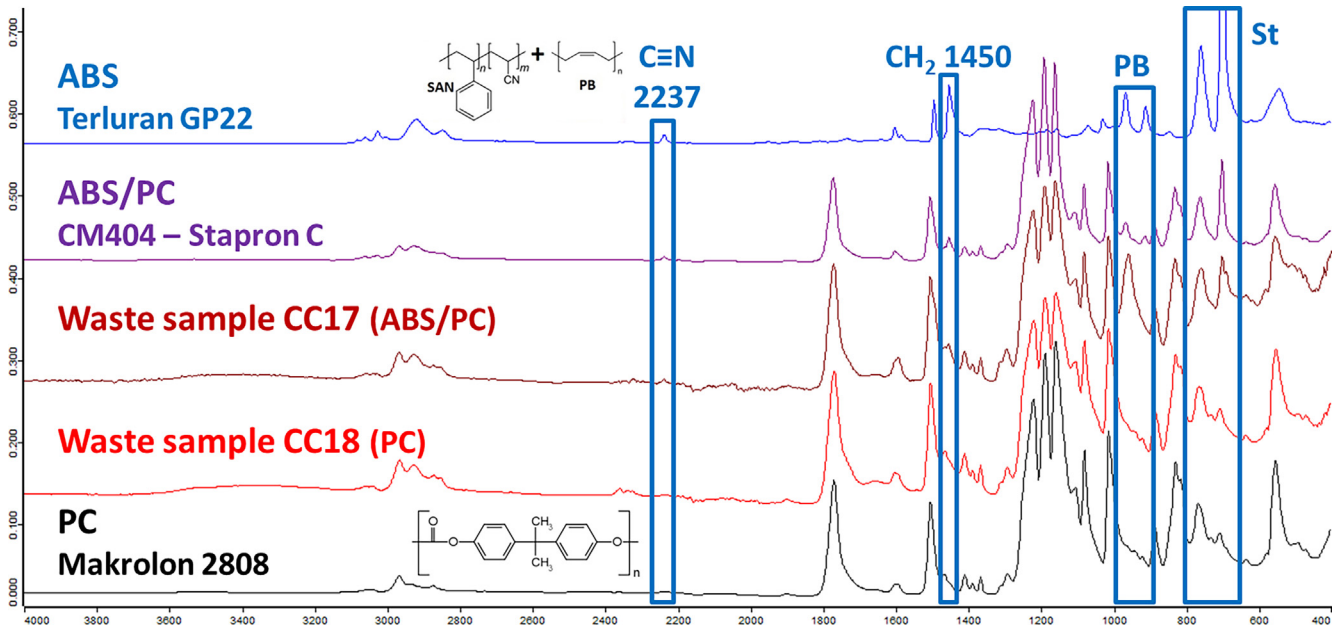

Fig. 11. MIR spectra comparison of ABS, ABS-PC and PC references to waste samples identified as ABS/PC and PC – visible ABS peaks in ABS-PC framed.

965 and 911, and CH_2 deformation at 1450 (just beyond LWIR), whereas PC only contains CH_3, aromatic hydrogens and hydroxyls.

In MWIR, the acrylonitrile peak at 2230 cm^{-1} is hardly visible in most real ABS-PC samples, especially with bad spectrum quality, because this signal is intrinsically weak, and ABS is the minor phase (Fig. 12). The signals from 3000 to 2800 cm^{-1} go through a convolution of signals of both ABS and PC and the resulting group gets more complex and the reference of ABS-PC pretty different, spectrally speaking, from its separated components. However, waste samples of ABS-PC and PC display spectra similar between each other but different from references of ABS-PC and PC. These differences could be explained by PC ageing, as O—H bands are visible from 3000 to 3300 and the carbonyl peak (central on Fig. 11) is widened at the base, concordantly to the photo-Fries mechanism (Collin et al., 2012; Rivaton, 1995). However, ageing studies rarely focus on aliphatic C—H stretching signals from 2800 to 3000 cm^{-1}. It seems improbable that the carbonate motif transformation impacts methyls which are separated from an aromatic cycle. Weak interactions between chains, which are rearranged because of ageing, are a more plausible explanation. Formulation is another one but no other "foreign" peak was spotted.

ABS-PMMA spectra of analyzed samples are closer to pure PMMA than pure ABS (Fig. 13), which can be explained by stronger absorption features of PMMA and low ABS amounts. This is coherent with the semi-transparency ("ABSTRON TIM 300 - Bhansali Engineering - datasheet," n.d.) of one waste sample issued from a vehicle light casing ("CG4" of Fig. 13). This could only be explained by a significant miscibility between SAN and PMMA (Lee et al., 1994) and negligible impact of PB nodules if they are grafted enough, small enough and few enough (Han and Yang, 1987; Kim et al., 1993).

Compared to PMMA, ABS-PMMA has a supplementary signal in MWIR range at 2330 because of acrylonitrile, also concerned by the same sensibility issue than in ABS-PC. Weak signals above 3000 associated with aromatic C-H stretching are also seen. The most notable difference in LWIR is the presence of the St signals at 700 (strong) and 760, whereas PMMA has a weaker signal at 750. Signals of PB can also be seen at 964, which is then stronger in ABS-PMMA than in pure PMMA. Finally, in the few analyzed PMMA samples, waste or references, the group of signals between 1000 and 1300 cm^{-1} displays a gap in its middle, which is not the case with ABS-PMMA samples. As with HIPS/GPPS or ABS/SAN,

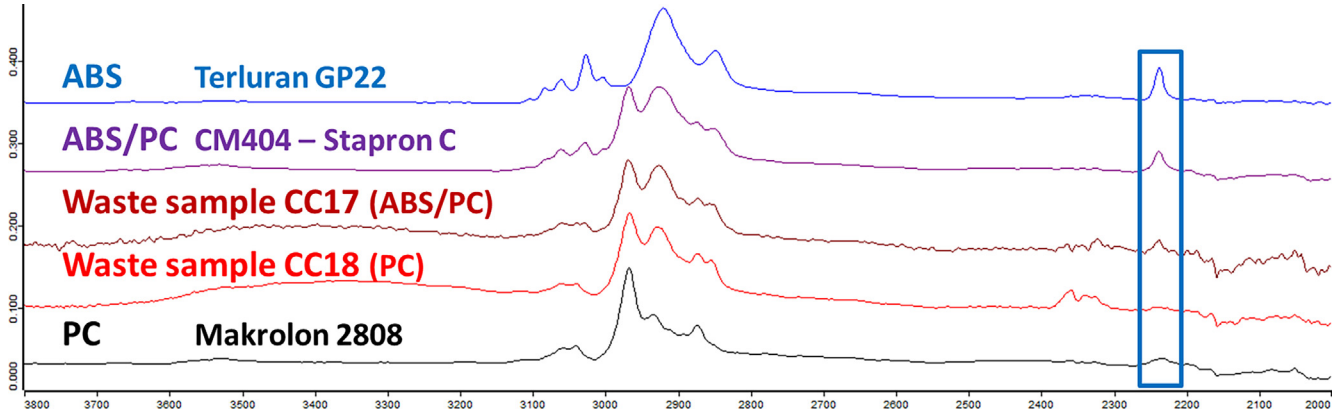

Fig. 12. MWIR spectra comparison of ABS, ABS-PC and PC references to waste samples identified as ABS-PC and PC – acrylonitrile peak characteristic of ABS framed in blue.

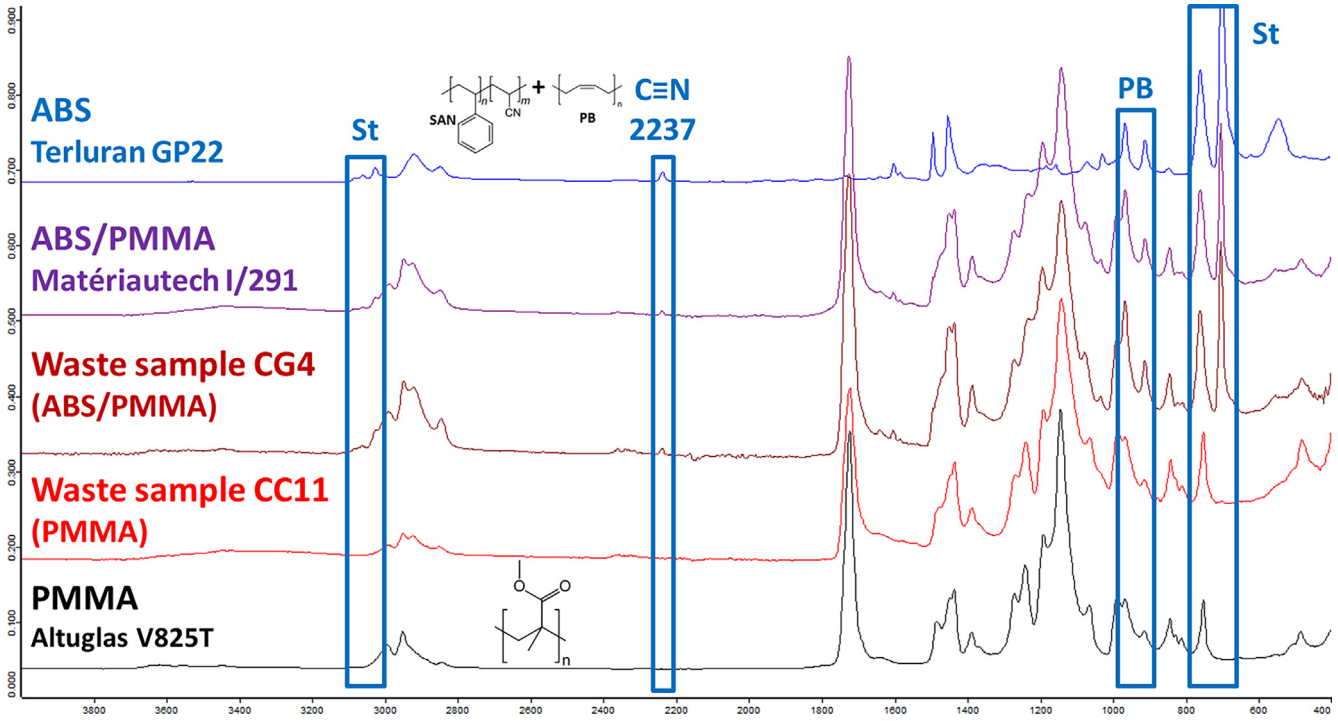

Fig. 13. MIR spectra comparison of waste samples identified as ABS-PMMA and PMMA to references of ABS, ABS-PMMA and PMMA – ABS peaks visible in ABS-PMMA framed.

ductility/fragility during cutting remove any doubt at laboratory scale for ABS-PMMA/PMMA or ABS-PC/PC differentiations. Surely for these impact resistance reasons, blends were found in majority in comparison to PC or PMMA alone. Mixing blends with respective components does not seem critical if only small amounts are added, especially for ABS-PC whose 30/70 ratio is an optimum.

About PMMA and PC differentiation, and thus, ABS-PMMA and ABS-PC differentiation, the first clue is the carbonyl peak wavenumber, at 1720 cm^{-1} for PMMA, at 1770, for PC. This higher value can be simply explained by the inductive effect of an oxygen atom on a carbonyl group. As PC present two oxygens as it is a carbonate instead of only one for PMMA, an ester, these effects are stronger. ASA carbonyl peak is at 1733 cm^{-1}, closer to PMMA as it is also acrylic. However, this signal is out of range for current HSI cameras.

In MWIR, PMMA has a 2990 signal which is rather distinctive, as said above, whereas the highest aliphatic C—H stretching peak (so below 3000) in PC is at 2970. In LWIR, the C—O stretching presents very different patterns. Indeed, PC displays with three close but very distinct peaks at 1220, 1190 and 1160 with growing heights. PMMA has four peaks from 1280 to 1060 with growing heights but they are closer and more convoluted than in PC, and as said above with or without a gap in the middle depending of the presence of ABS. As discussed with HIPS-PPE, LWIR signal richness could be a handicap for convolution and data managing issues.

4. Conclusion

Characteristic signals of various types of styrenic polymers enabled to build tools to help Mid Infrared spectral identification at both laboratory and industrial scales. Hyperspectral Imagery cameras present far weaker wavelength ranges and resolution for technological reasons. High output, necessary in an industrial context, also demands acquisition times in the order of the millisecond, whereas laboratory equipment takes often several seconds. Styrenic materials are the majority of WEEE plastics which are often colored with carbon black, preventing NIR HSI sorting. Moreover, their densities overlap, preventing sink-float sorting. Thus, MIR (4000–400 cm^{-1}) spectral features of styrenics were finely described as every signal can be discriminant in the limited conditions of MIR HSI. In the MWIR range (5000–2000 cm^{-1}), they present several rather weak but visible signals in the 3100–3000 range corresponding to aromatic hydrogens. They also display two large signals at 2920 and 2850. Acrylonitrile signal at 2235 cm^{-1} is very specific of ABS. In LWIR (≈1350–700 cm^{-1}), the two aromatic C—H bending signals are very specific, with 750 and 695 values for PS based polymers, and with 760 and 700 for SAN based polymer. Differentiation between GPPS and HIPS, and between SAN and ABS, which relies on the presence of PB, cannot be reliably detected through infrared surface analysis. However, this should not present compatibility issues.

ASA is very distinguishable because of the acrylic nature of its rubbery phase. α-methylstyrene which can be copolymerized to styrenics to enhance their thermal properties, adds a hardly detectable peak at 1375. HIPS-PPE blend is easily differentiated from HIPS in LWIR, but hardly in MWIR, especially in degraded conditions. ABS-PC and ABS-PMMA spectra are rather close to PC and PMMA with small additional peaks which can be hard to detect even at laboratory scale. PC and PMMA are easily differentiated in MWIR, where PMMA has stronger and higher aliphatic C-H stretching peaks, and in LWIR with very rich and very different C-O stretching patterns between 1300 and 1000 cm^{-1}. The carbonyl stretching wavelength is very discriminatory between them but out of range for current HSI cameras. In general, LWIR contains more signals but this abundance which can facilitate identification can also be a drawback as peaks can convolve and this means more data handling in the short acquisition-treatment time necessary in industrial conditions.

With spectral comparison to a hundred of real waste samples, it was found that wavenumbers are really characteristic within the used resolution and a difference out of this range is probably significant of a chemical difference. It is also important to use several peaks to identify a polymer and double-check its nature. For exam-

ple, PC blended to ABS should not be identified with only the 1770 cm^{-1} signal, but also at least with the three equally strong signals from 1300 to 1000 and a 1760 signal cannot be associated to PC. Other distinctions will not be applicable at industrial scale in a near future, because of too subtle differences for weaker resolutions or for being out of range for HSI cameras. These considerations are thus important for waste management, especially mechanical recycling, as they highlight the limits of sorting and consequently the natures of impurities which could still be in the corresponding waste streams after sorting. By knowing impurity natures and amounts, one could plan more relevant and reliable compatibilization strategies to enable best achievable properties for secondary raw materials. Further works on other materials, especially polyolefins, laboratory degraded acquisition, formulation, especially mineral fillers and carbon black, and polymer ageing will also help completing the whole frame to support development of maximal identification at both laboratory and industrial scales.

Funding

This work was supported by BPI France via the FUI 20 (Fonds Unique Interministériel) grant.

Acknowledgements

The authors would like to thank Benjamin Gallard and Robert Lorquet for technical support, respectively for polymer processing and spectroscopy experiments. Suez and Pellenc ST are gratefully acknowledged for partnership in this work. Finally, the authors are very thankful to Materiautech from Allizé-Plasturgie for providing the half of the references used in this work.

Appendix A and B. Supplementary material

Supplementary data to this article can be found online at https://doi.org/10.1016/j.wasman.2019.05.050.

References

ABSTRON TIM 300 - Bhansali Engineering - datasheet [WWW Document], n.d. URL https://omnexus.specialchem.com/product/t-bhansali-engineering-abstron-tim-300 (Accessed 1.12.18).

Alfarraj, A., Bruce Nauman, E., 2004. Super HIPS: improved high impact polystyrene with two sources of rubber particles. Polymer (Guildf). 45, 8435–8442. https://doi.org/10.1016/j.polymer.2004.10.005.

Allizé-Plasturgie: a professional organisation at the service of plastics and composites | Allizé-Plasturgie [WWW Document], n.d. URL https://www.allize-plasturgie.org/allize-plasturgie-professional-organisation-service-plastics-and-composites (Accessed 12.3.18).

Ángel Aguirre, M., Hidalgo, M., Canals, A., Nóbrega, J.A., Pereira-Filho, E.R., 2013. Analysis of waste electrical and electronic equipment (WEEE) using laser induced breakdown spectroscopy (LIBS) and multivariate analysis. Talanta 117, 419–424. https://doi.org/10.1016/j.talanta.2013.09.046.

Aquino, F.W.B., Pereira-Filho, E.R., 2015. Analysis of the polymeric fractions of scrap from mobile phones using laser-induced breakdown spectroscopy: Chemometric applications for better data interpretation. Talanta 134, 65–73. https://doi.org/10.1016/j.talanta.2014.10.051.

Arnold, J.C., Alston, S., Holder, A., 2009. Void formation due to gas evolution during the recycling of Acrylonitrile–Butadiene–Styrene copolymer (ABS) from waste electrical and electronic equipment (WEEE). Polym. Degrad. Stab. 94, 693–700. https://doi.org/10.1016/j.polymdegradstab.2008.12.019.

Barbier, S., Perrier, S., Freyermuth, P., Perrin, D., Gallard, B., Gilon, N., 2013. Plastic identification based on molecular and elemental information from laser induced breakdown spectra: A comparison of plasma conditions in view of efficient sorting. Spectrochim. Acta - Part B At. Spectrosc. 88, 167–173. https://doi.org/10.1016/j.sab.2013.06.007.

Beigbeder, J., Perrin, D., Mascaro, J.-F., Lopez-Cuesta, J.-M., 2013. Study of the physico-chemical properties of recycled polymers from waste electrical and electronic equipment (WEEE) sorted by high resolution near infrared devices. Resour. Conserv. Recycl. 78, 105–114. https://doi.org/10.1016/j.resconrec.2013.07.006.

BIR - Bureau of International Recycling - E-Scrap [WWW Document], n.d. URL http://www.bir.org/industry/escrap/?locale=en_US (Accessed 5.3.18).

Censori, M., La Marca, F., Carvalho, M.T., 2016. Separation of plastics: The importance of kinetics knowledge in the evaluation of froth flotation. Waste Manag. 54, 39–43. https://doi.org/10.1016/j.wasman.2016.05.021.

Collin, S., Bussière, P.-O., Thérias, S., Lambert, J.-M., Perdereau, J., Gardette, J.-L., 2012. Physicochemical and mechanical impacts of photo-ageing on bisphenol a polycarbonate. Polym. Degrad. Stab. 97, 2284–2293. https://doi.org/10.1016/j.polymdegradstab.2012.07.036.

Costa, V.C., Aquino, F.W.B., Paranhos, C.M., Pereira-Filho, E.R., 2017. Identification and classification of polymer e-waste using laser-induced breakdown spectroscopy (LIBS) and chemometric tools. Polym. Test. 59, 390–395. https://doi.org/10.1016/j.polymertesting.2017.02.017.

Dobrovszky, K., Ronkay, F., 2014. Alternative polymer separation technology by centrifugal force in a melted state. Waste Manag. 34, 2104–2112. https://doi.org/10.1016/j.wasman.2014.05.006.

Forest, C., Chaumont, P., Cassagnau, P., Swoboda, B., Sonntag, P., 2015. Generation of nanocellular foams from ABS terpolymers. Eur. Polym. J. 65, 209–220. https://doi.org/10.1016/j.eurpolymj.2014.11.006.

Greco, R., Astarita, M.F., Dong, L., Sorrentino, A., 1994. Polycarbonate/ABS blends: Processability, thermal properties, and mechanical and impact behavior. Adv. Polym. Technol. 13, 259–274. https://doi.org/10.1002/adv.1994.060130402.

Grégoire, S., Boudinet, M., Pelascini, F., Surma, F., Detalle, V., Holl, Y., 2011. Laser-induced breakdown spectroscopy for polymer identification. Anal. Bioanal. Chem. 400, 3331–3340. https://doi.org/10.1007/s00216-011-4898-2.

Gu, F., Ma, B., Guo, J., Summers, P.A., Hall, P., 2017. Internet of things and Big Data as potential solutions to the problems in waste electrical and electronic equipment management: An exploratory study. Waste Manag. 68, 434–448. https://doi.org/10.1016/j.wasman.2017.07.037.

Gundupalli, S.P., Hait, S., Thakur, A., 2017. A review on automated sorting of source-separated municipal solid waste for recycling. Waste Manag. 60, 56–74. https://doi.org/10.1016/j.wasman.2016.09.015.

Hamad, K., Kaseem, M., Deri, F., 2013. Recycling of waste from polymer materials: An overview of the recent works. Polym. Degrad. Stab. 98, 2801–2812. https://doi.org/10.1016/j.polymdegradstab.2013.09.025.

Han, C.D., Yang, H.-H., 1987. Rheological behavior of blends of poly(methyl methacrylate) (PMMA) and poly(acrylonitrile-stat-styrene)-graft-polybutadiene (ABS). J. Appl. Polym. Sci. 33, 1221–1229. https://doi.org/10.1002/app.1987.070330413.

Huang, J., Tian, C., Ren, J., Bian, Z., 2017. Study on impact acoustic—visual sensor-based sorting of ELV plastic materials. Sensors 17, 1325. https://doi.org/10.3390/s17061325.

Huber, N., Eschlböck-Fuchs, S., Scherndl, H., Freimund, A., Heitz, J., Pedarnig, J.D., 2014. In-line measurements of chlorine containing polymers in an industrial waste sorting plant by laser-induced breakdown spectroscopy. Appl. Surf. Sci. 302, 280–285. https://doi.org/10.1016/j.apsusc.2013.10.070.

Kassouf, A., Maalouly, J., Rutledge, D.N., Chebib, H., Ducruet, V., 2014. Rapid discrimination of plastic packaging materials using MIR spectroscopy coupled with independent components analysis (ICA). Waste Manag. 34, 2131–2138. https://doi.org/10.1016/j.wasman.2014.06.015.

Kim, Y.J., Shin, G.S., Lee, I.T., Kim, B.K., 1993. Miscible and immiscible blends of ABS with PMMA. I. Morphology and rheology. J. Appl. Polym. Sci. 47, 295–304. https://doi.org/10.1002/app.1993.070470209.

Kister, G., Cassanas, G., Vert, M., 1998. Effects of morphology, conformation and configuration on the IR and Raman spectra of various poly(lactic acid)s. Polymer (Guildf). 39, 267–273. https://doi.org/10.1016/S0032-3861(97)00229-2.

Langhals, H., Zgela, D., Schlücker, T., 2014. High performance recycling of polymers by means of their fluorescence lifetimes. Green Sustain. Chem. 04, 144–150. https://doi.org/10.4236/gsc.2014.43019.

Lee, S.M., Choi, C.H., Kim, B.K., 1994. Effect of matrix SAN in ABS/PMMA blends. J. Appl. Polym. Sci. 51, 1765–1770. https://doi.org/10.1002/app.1994.070511009.

Mooney, J.M., Vickers, V.E., An, M., Brodzik, A.K., 1997. High-throughput hyperspectral infrared camera. J. Opt. Soc. Am. A 14, 2951. https://doi.org/10.1364/JOSAA.14.002951.

Peeters, J.R., Vanegas, P., Kellens, K., Wang, F., Huisman, J., Dewulf, W., Duflou, J.R., 2015. Forecasting waste compositions: A case study on plastic waste of electronic display housings. Waste Manag. 46, 28–39. https://doi.org/10.1016/j.wasman.2015.09.019.

Peeters, J.R., Vanegas, P., Tange, L., Van Houwelingen, J., Duflou, J.R., 2014. Closed loop recycling of plastics containing Flame Retardants. Resour. Conserv. Recycl. 84, 35–43. https://doi.org/10.1016/j.resconrec.2013.12.006.

Pérez-Belis, V., Bovea, M., Ibañez-Forés, V., 2015. An in-depth literature review of the waste electrical and electronic equipment context: Trends and evolution. Waste Manag. Res. 33, 3–29. https://doi.org/10.1177/0734242X14557382.

Perrin, D., Mantaux, O., Ienny, P., Léger, R., Dumon, M., Lopez-Cuesta, J.M., 2016. Influence of impurities on the performances of HIPS recycled from Waste Electric and Electronic Equipment (WEEE). Waste Manag. 56, 438–445. https://doi.org/10.1016/j.wasman.2016.07.014.

PlasticsEurope Market Research Group (PEMRG)/Consultic Marketing & Industrieberatung GmbH, 2017. Plastics – the Facts 2017 16.

Pongstabodee, S., Kunachitpimol, N., Damronglerd, S., 2008. Combination of three-stage sink–float method and selective flotation technique for separation of mixed post-consumer plastic waste. Waste Manag. 28, 475–483. https://doi.org/10.1016/j.wasman.2007.03.005.

Ragaert, K., Delva, L., Van Geem, K., 2017. Mechanical and chemical recycling of solid plastic waste. Waste Manag. 69, 24–58. https://doi.org/10.1016/j.wasman.2017.07.044.

Rivaton, A., 1995. Recent advances in bisphenol-A polycarbonate photodegradation. Polym. Degrad. Stab. 49, 163–179. https://doi.org/10.1016/0141-3910(95)00069-X.

Roh, S.-B., Oh, S.-K., Park, E.-K., Choi, W.Z., 2017. Identification of black plastics realized with the aid of Raman spectroscopy and fuzzy radial basis function neural networks classifier. J. Mater. Cycles Waste Manag. 19, 1093–1105. https://doi.org/10.1007/s10163-017-0620-6.

Rozenstein, O., Puckrin, E., Adamowski, J., 2017. Development of a new approach based on midwave infrared spectroscopy for post-consumer black plastic waste sorting in the recycling industry. Waste Manag. 68, 38–44. https://doi.org/10.1016/j.wasman.2017.07.023.

Salhofer, S., Steuer, B., Ramusch, R., Beigl, P., 2016. WEEE management in Europe and China – A comparison. Waste Manag. 57, 27–35. https://doi.org/10.1016/j.wasman.2015.11.014.

Saviello, D., Pouyet, E., Toniolo, L., Cotte, M., Nevin, A., 2014. Synchrotron-based FTIR microspectroscopy for the mapping of photo-oxidation and additives in acrylonitrile-butadiene-styrene model samples and historical objects. Anal. Chim. Acta 843, 59–72. https://doi.org/10.1016/j.aca.2014.07.021.

Serranti, S., Gargiulo, A., Bonifazi, G., 2011. Characterization of post-consumer polyolefin wastes by hyperspectral imaging for quality control in recycling processes. Waste Manag. 31, 2217–2227. https://doi.org/10.1016/j.wasman.2011.06.007.

Serranti, S., Gargiulo, A., Bonifazi, G., 2010. The utilization of hyperspectral imaging for impurities detection in secondary plastics. Open Waste Manag. J. 3, 56–70. https://doi.org/10.2174/1876400230100301056.

Soo, V.K., Doolan, M., 2014. Recycling mobile phone impact on life cycle assessment. Procedia CIRP 15, 263–271. https://doi.org/10.1016/j.procir.2014.06.005.

Tolue, S., Moghbeli, M.R., Ghafelebashi, S.M., 2009. Preparation of ASA (acrylonitrile-styrene-acrylate) structural latexes via seeded emulsion polymerization. Eur. Polym. J. 45, 714–720. https://doi.org/10.1016/j.eurpolymj.2008.12.014.

Utracki, L.A., 1998. Commercial Polymer Blends. Springer, US, Boston, MA. https://doi.org/10.1007/978-1-4615-5789-0.

Vilaplana, F., Ribes-Greus, A., Karlsson, S., 2006. Degradation of recycled high-impact polystyrene. Simulation by reprocessing and thermo-oxidation. Polym. Degrad. Stab. 91, 2163–2170. https://doi.org/10.1016/j.polymdegradstab.2006.01.007.

Vrancken, C., Longhurst, P.J., Wagland, S.T., 2017. Critical review of real-time methods for solid waste characterisation: Informing material recovery and fuel production. Waste Manag. 61, 40–57. https://doi.org/10.1016/j.wasman.2017.01.019.

Wang, J., Wang, Y., Liu, J., Zhang, S., Zhang, M., 2018. Effects of fund policy incorporating extended producer responsibility for WEEE dismantling industry in China. Resour. Conserv. Recycl. 130, 44–50. https://doi.org/10.1016/j.resconrec.2017.11.016.

Wypych, G., 2016a. ABS Poly(acrylonitrile-co-butadiene-co-styrene). In: Handbook of Polymers. Elsevier, pp. 5–11. https://doi.org/10.1016/B978-1-895198-92-8.50005-7.

Wypych, G., 2016b. PPO poly(phenylene oxide). In: Handbook of Polymers. Elsevier, pp. 522–525. https://doi.org/10.1016/B978-1-895198-92-8.50162-2.

Yamaji, Y., Okaya, K., Dodbiba, G., Wang, L.P., Fujita, T., 2013. A novel separation method for plastic of discarded appliance including black plastic by using Raman spectroscopy. Resour. Process. 60, 65–71. https://doi.org/10.4144/rpsj.60.65.

Yee, A.F., 1977. Mechanical properties of mixtures of two compatible polymers. Polym. Eng. Sci. 17, 213–219. https://doi.org/10.1002/pen.760170310.

Yuan, H., Fu, S., Tan, W., He, J., Wu, K., 2015. Study on the hydrocyclonic separation of waste plastics with different density. Waste Manag. 45, 108–111. https://doi.org/10.1016/j.wasman.2015.01.037.